Terra Nova

doi: 10.1111/ter.12218

Temporal and bathymetric resolution of nautiloid death assemblages in stratigraphically condensed oozes (New Caledonia)

Adam Tomašových,[1] Ján Schlögl,[2] Darrell S. Kaufman[3] and Natália Hudáčková[2]

[1]*Earth Science Institute, Slovak Academy of Sciences, Dubravska cesta 9, Bratislava 84005, Slovakia;* [2]*Department of Geology and Paleontology, Comenius University, Mlynska dolina G, Bratislava 84215, Slovakia;* [3]*School of Earth Sciences & Environmental Sustainability, Northern Arizona University, Campus Box 4099, Flagstaff, AZ 86011, USA*

ABSTRACT

Cephalopod shells can be affected by postmortem transport and biostratigraphic condensation, but direct estimates of the temporal and spatial resolutions of cephalopod assemblages are missing. Amino acid racemisation calibrated by ^{14}C demonstrates a centennial-scale time averaging (<500 years) of *Nautilus macromphalus* in sediment-starved, epi- and mesobathyal pelagic environments. The few shells that are thousands of years old are highly degraded. The median occurrence of dead shells is at 445 m depth, close to the 300–400 m depth where living *N. macromphalus* are most abundant. Therefore, dead shells of this species accumulate at a centennial temporal resolution and with excellent bathymetric fidelity. Dead *Nautilus* shells exist for only a few hundred years on the seafloor, in contrast to the biostratigraphically condensed mixture of extant foraminifers and foraminifers that went extinct during the Pleistocene. Cephalopod shells that do not show any signs of early diagenetic cementation are unlikely to be biostratigraphically condensed.

Terra Nova, 00: 1–8, 2016

Introduction

Chambered cephalopods frequently show rapid evolutionary turnover and attain broad geographic ranges, and thus represent one of the key groups used in high-resolution stratigraphic, biogeographic and oceanographic inferences of fossil assemblages (Brayard *et al*., 2006; Dera *et al*., 2011; Sessa *et al*., 2015). However, chambered cephalopods can be subjected to postmortem ascent and significant drift by water currents, thus confounding interpretations of environmental conditions and biogeographic distribution (Fernández-López and Meléndez, 1996; Chirat, 2000). Chambered cephalopods are also subject to significant condensation because they frequently inhabited open-shelf and pelagic-swell environments that were prone to sediment starvation in the past (Wendt and Aigner, 1985; Santantonio and Carminati, 2011; Coimbra and Olóriz, 2012). Present-day species of *Nautilus* predominantly inhabit bathyal environments with ooze deposition in the Indo-Pacific. Such environments are characterised by sediment starvation, by ferromanganeous and glauconitic deposits that grow in the absence of sedimentation at millennial to million-year timescales (Föllmi, 2016), and by a co-occurrence of extant and Pleistocene foraminifers that implies significant stratigraphic condensation (Hayward and Kagawata, 2005). We suggest that present-day sediment-starved pelagic environments can provide taphonomic windows into processes that generated biostratigraphically condensed assemblages in the past.

Here, we quantify the temporal and bathymetric resolutions of nautiloid death assemblages in such sediment-starved environments. First, we estimate postmortem age with ^{14}C and amino acid racemisation in 26 shells of *N. macromphalus* collected in bathyal environments off New Caledonia to constrain their rate of disintegration on the seafloor and thus their potential for stratigraphic condensation. Second, we show that some calcitic foraminifers extracted from sediment infills of *Nautilus* shells went extinct during the Pleistocene, thus providing information on significant differences in time averaging between nautiloid and foraminiferal assemblages.

Correspondence: Adam Tomašových, Earth Science Institute, Slovak Academy of Sciences, Dubravska cesta 9, Bratislava 84005, Slovakia. Tel.: +0421 904 852145; e-mail: geoltoma@savba.sk

Methods

Twenty-one dead shells of *N. macromphalus* were sampled with beam trawls and dredges at eleven sites around the New Caledonia archipelago in 1985 and 1987 (Fig. S1, Table S1, De Forges, 1990). Five additional specimens sampled between New Caledonia and the Chesterfield Islands in 2003 and 2005 were described by Mapes *et al*. (2010a). Eighteen shells were collected between 330 and 750 m depth in the epibathyal zone, and eight shells were collected between 750 and 2045 m in the mesobathyal zone. Seawater temperature off New Caledonia between 300 m and 600 m depth declines from 15 to 5 °C, and is 4 °C at 1000 m (Roux *et al*., 1991). We split the shells into epibathyal and mesobathyal assemblages to reduce the effect of temperature on the rate of racemisation. Fourteen shells contained ooze sediment that was wet sieved with a 0.071 mm mesh size. We identified 250 foraminifer specimens to species level in each of these shells, and determined their last stratigraphic appearance datum.

The ages of seven specimens dated with ^{14}C at the AMS facility at the Poznan Radiocarbon Laboratory were converted to calendar years using the Marine13 data and Calib7.1 (Stuiver and Reimer, 1993), with a regional marine reservoir correction (ΔR) equal to 26 years (SD = 23 years) (Table S2). The ^{14}C activity of one specimen (CP30/4) was indistinguishable from background levels, implying an age of at least 50 000 years.

The outermost chamber whorls were split into external spherulitic-prismatic and middle nacreous layers, which were analysed separately for the extent of amino acid racemisation (AAR) using reverse-phase high-pressure liquid chromatography analysis (Kaufman and Manley, 1998). We screened the data according to Kosnik and Kaufman (2008) and calibrated the rate of AAR according to Allen *et al.* (2013) with seven specimens (including one specimen dated by ^{210}Pb in Mapes *et al.*, 2010a) (Figs S2 and S3), fitting aspartic (Asp) and glutamic (Glu) acid D/L values separately for each layer (Fig. 1A,B and Table S3).

Postmortem ages estimated on the basis of nacreous and prismatic layers are similar (Fig. 1C). In addition to the ^{14}C and ^{210}Pb ages of eight shells, the AAR ages of the additional 18 shells used in the analyses of temporal resolution are derived from the nacreous layer, which shows a larger covariation in the extents of racemisation among amino acids and is less affected by microbioerosion than the prismatic layer (Figs S4 and S5). All ages refer to time since sampling of shells on the seafloor (Table S4). To quantify the rate of loss of *Nautilus* shells from the surface seafloor sediments on the basis of two depth-specific age–frequency distributions (AFDs), we used a simple exponential model (rate of loss is constant in time), a Weibull model (rate of loss gradually declines over time, e.g. old shells disintegrate at a slower rate than young shells), and a two-phase exponential model (rate of loss abruptly declines over time) (Tomašových *et al.*, 2014).

Results

The AFD of *N. macromphalus* is strongly right-skewed, with a median age of 263 years and an interquartile range (IQR) of 394 years (Fig. 2). Twenty specimens are younger than 500 years and six specimens are older than 1000 years (Table S1). Three specimens older than 1000 years were found at 1140 m depth. The AFD from the epibathyal zone is similarly characterised by centennial-scale time averaging (median = 260 years and IQR = 220 years). The AFD from the mesobathyal zone shows a similar median age (363 years) but the IQR is equal to ~2000 years due to the presence of one very old specimen (older than ~50 000 years). The mixture of frequent young shells (younger than 500 years) and rare very old shells best supports the two-phase exponential and Weibull models of skeletal loss in both depth-specific assemblages and in the entire collection, implying a decline in the rate of shell disintegration from centennial- (195 years) to millennial-scale half-lives (3013 years) while shells are exposed in the mixed layer (Table S5). The shells older than 1000 years are highly incomplete, with relicts of walls and umbilicum (Fig. 2); and incompleteness of phragmocones correlates positively with postmortem age (Spearman $r = 0.77$, $P < 0.0001$, Fig. S6). Shells are frequently penetrated by microborings (Fig. 3A,B). Some specimens show μm-thick, yellowish to brownish aggregates of clays, goethite (determined by X-ray diffraction), and coccoliths that coat empty borings and external surfaces (Fig. 3C,D). However, tabular aragonitic crystallites forming the nacreous layer do not show any signs of diagenetic cementation (Fig. 3E,F), and the internal sediment within the whorls is never lithified.

Of the sediment samples extracted from the whorls of 14 shells, 13 contained at least one foraminifer species that went extinct during the Pleistocene (Table S1). These extinct species co-occur with extant species, thus showing significant million-year-scale time averaging. They include the pink *Globigerinoides rubra* that went extinct in the Pacific 120 000 years ago (Thompson *et al.*, 1979), the planktonic species *Sphaeroidinellopsis paenedehiscens, Globigerinoides fistulosus* and *Pulleniatina praecursor* that went extinct during the Lower Pleistocene at the end of the Gelasian 1.9–1.8 Ma ago

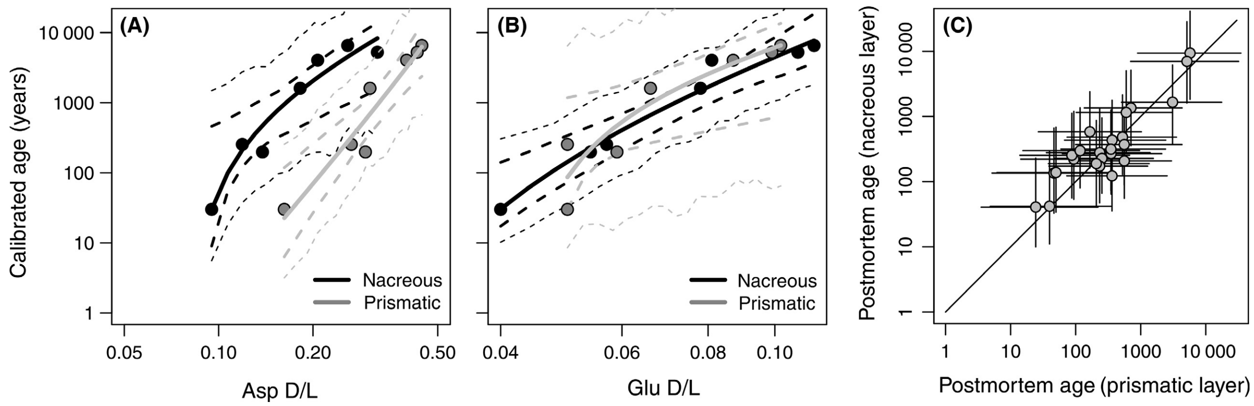

Fig. 1 (A,B) The relation between postmortem calendar age (estimated by AMS) and the *D*/*L* values of two amino acids for the prismatic and nacreous layers, best-fit by the apparent parabolic kinetic model, with 95% prediction intervals (dashed lines). (C) Calibrated postmortem ages correlate highly between the nacreous and prismatic layers. Error bars represent 95% prediction intervals on age estimates.

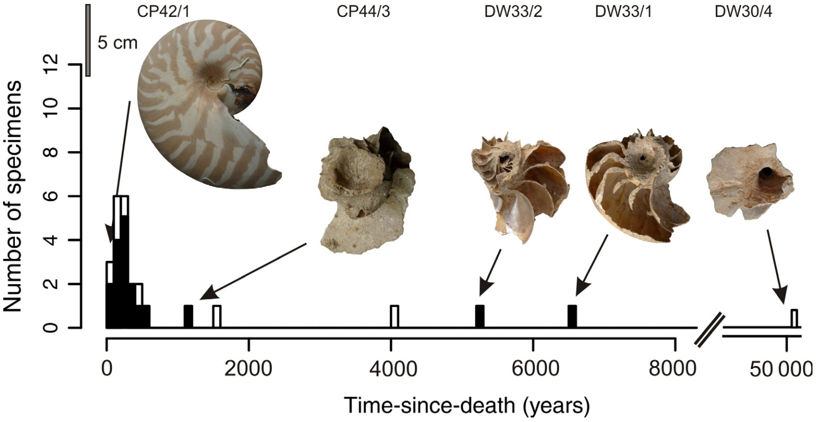

Fig. 2 Postmortem age–frequency distribution (AFD) of *Nautilus macromphalus*, with dark bars representing epibathyal specimens found at depths shallower than 750 m, and white bars representing mesobathyal specimens found at depths deeper than 750 m.

(Kennett and Srinivasan, 1983), and benthic genera *Strictocostella* and *Siphonodosaria* of the family Stilostomellidae that went extinct during the mid-Pleistocene event 0.8–0.53 Ma ago (Hayward *et al*., 2012) (Fig. 4, Table S1). Although the total number of all determined foraminifers (3500 specimens) is much larger than the number of *Nautilus* shells, the total age range predicted for *Nautilus* by the two-phase model for 3500 specimens would be ~30 000 years (IQR = 490 years) (Table S5). Therefore, the difference in time averaging between aragonitic cephalopods (centuries to a few thousand years) and calcitic foraminifers (*c*. 2 Ma) cannot be explained by differences in sample size.

The median depth of dead individuals of *N. macromphalus* is 445 m, and the median depth of stations at which dead individuals were found is 440 m, with most individuals collected above 800 m and few individuals below 1000 m. In contrast, the 306 grab and dredge collections (i.e. not just the collections that contain shells of *N. macromphalus*) sampled during the Biocal and Biogeocal

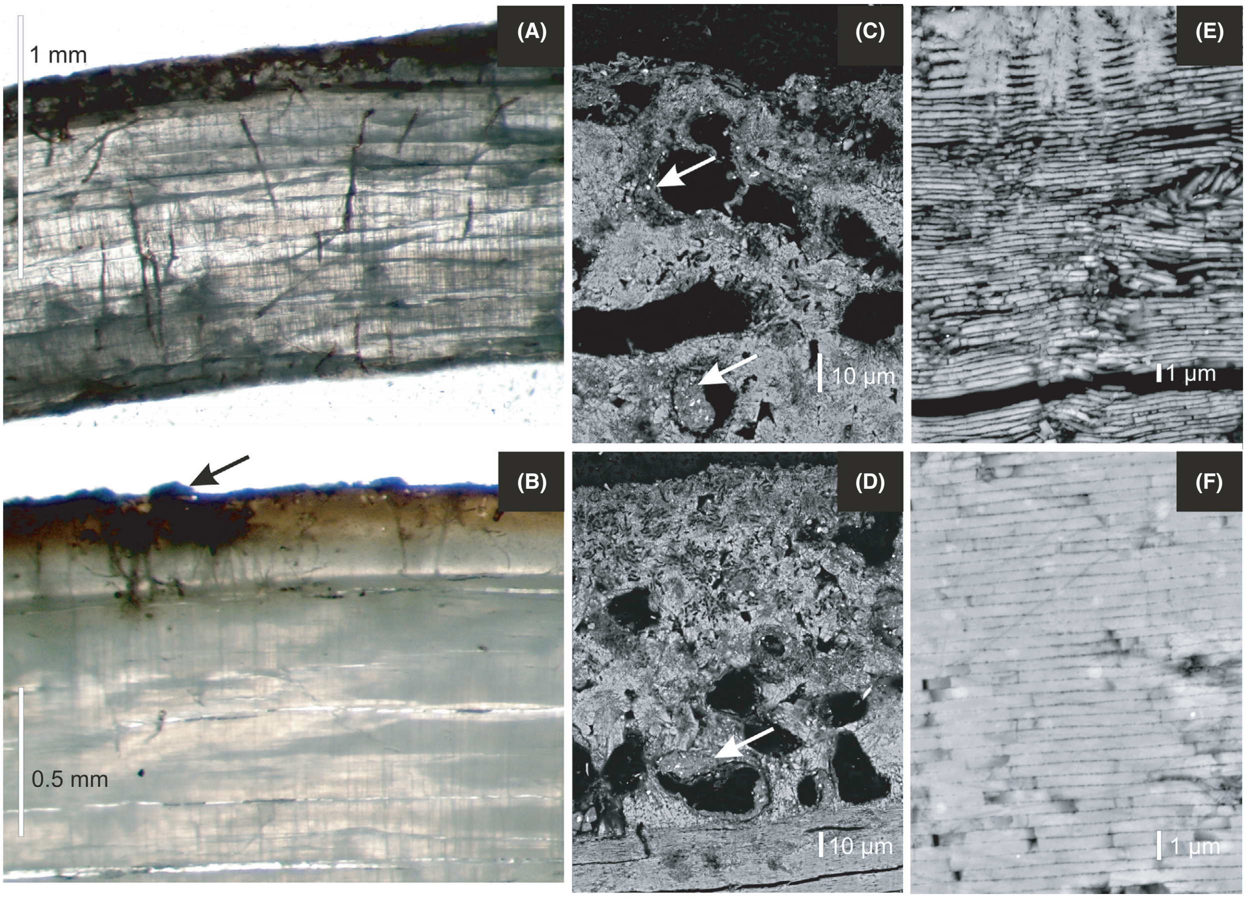

Fig. 3 (A,B) Light-microscope photographs showing (A) penetration of the prismatic and nacreous layers by dark-stained microborings (specimen CP 232) and (B) discontinuous coatings (black arrow) and microboring infills (CP272). (C,D) Backscattered electron (BSE) images showing thin goethite-clay aggregates rich in coccoliths (white arrows) that coat microborings (CP232). (E,F) BSE images showing well-preserved tables of the nacreous layer with no signs of recrystallisation (CP232).

campaigns in 1985 and 1987 have a median depth of 1478 m and a mode of 2400 m (Fig. 5). Therefore, the bathymetric distribution of the collections containing dead shells of *N. macromphalus* does not match the distribution of all the samples collected in the cruise campaigns. Dead shells of *N. macromphalus* thus occur at significantly shallower water depths than would be expected under significant postmortem dispersal, which should increase the bathymetric range of dead shells.

Discussion

The shape of the AFD in surficial seafloor sediments depends on shell disintegration, on shell burial and exhumation within the mixed layer and on burial of shells below the mixed layer (Tomašových *et al.*, 2014; Olszewski and Kaufman, 2015; Terry and Novak, 2015), assuming steady-state production over the course of the last few thousand years (Tomašových *et al.*, 2016). This assumption is supported by findings of frequent shells of *N. macromphalus* in caves off Lifou Islands that are ~6000 years old (Landman *et al.*, 2014), and by relatively stable conditions with near-modern seawater temperature occurring in New Caledonia for the last few thousand years (Cabioch, 2003; Gagan *et al.*, 2004). Sediment accumulation rates seem to be extremely slow to zero because surface sediments with dead shells of nautiloids on current-swept block-faulted slopes off New Caledonia are dominated by erosion and sediment bypassing (Roux *et al.*, 1991). We thus suggest that the loss rates estimated by the two-phase exponential model reflect disintegration rates of *N. macromphalus* on the seafloor because sedimentological conditions and co-occurrence of Recent foraminifers with relict Pleistocene foraminifers imply long residence times of cephalopod remains on the seafloor. Under such conditions, condensed surface sediments or exhumed subsurface sediments with older foraminifers can be winnowed by bottom currents and trapped by the whorls (Maeda, 1991) or by the depressed umbilical regions (Henderson and McNamara, 1985).

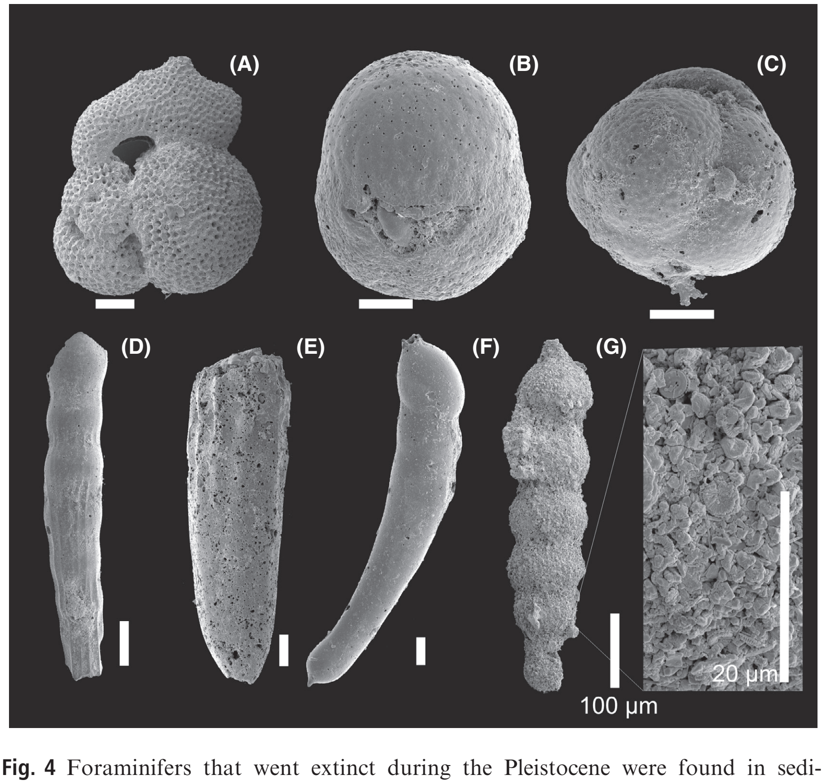

Fig. 4 Foraminifers that went extinct during the Pleistocene were found in sediments within shells of *N. macromphalus*. (A) *Globigerinoides fistulosus* Schubert 1910, CP30; (B) *Sphaeroidinellopsis paenedehiscens* Blow, 1969, CP272; (C) *Pulleniatina praecursor*, CP272; (D) *Strictocostella* sp., DW44/3; (E) *Strictocostella* sp., DW43; (F) *Strictocostella scharbergana* Neugeboren 1856, DW 45/1, (G) *Siphonodosaria lepidula* Schwager 1886, DW 33/2. The inset shows that the test is coated by a coccolith-rich crust.

Environmental variation in skeletal disintegration rates (Kidwell *et al.*, 2005; Powell *et al.*, 2011) can confound estimates of disintegration, which can be particularly faster in depths exceeding 1000 m due to the proximity of the aragonite compensation depth at 1100–1200 m in this region (Feely *et al.*, 2002). However, the centennial-scale time averaging, the time-declining disintegration rate and its magnitude are robust to the exclusion of mesobathyal shells (Table S5). Water depth does not correlate with postmortem age (Spearman $r = 0.2$, $P = 0.33$), and three specimens older than 1000 years occur at depth 1140 m, implying that disintegration half-lives at such depths are comparable to those at epibathyal depths. The preservation model with temporally declining shell disintegration rate can be explained by a higher durability of relict specimens because umbilical walls increase in thickness and the density of septal walls also increases towards the central part of the phragmocone.

The bathyal setting around New Caledonia is sedimentologically and taphonomically analogous to Paleozoic and Mesozoic sediment-starved pelagic swells. First, sediments are dominated by pteropods and planktonic foraminifers below 200 m and up to 2000 m off New Caledonia (Cotillon *et al.*, 1989); in the same way, pelagic-swell successions with condensed deposits are dominated by pelagic producers rather than by carbonate input from shallow platforms (Martire, 1996). Second, the external coatings and microboring infills formed by a mixture of goethite and clays observed here could be precursors of glauconitic infills or iron-stained crusts that are characteristic signatures of skeletal preservation in condensed successions (Martin-Algarra and Sanchez-Navas, 1995; Pavia *et al.*, 2013).

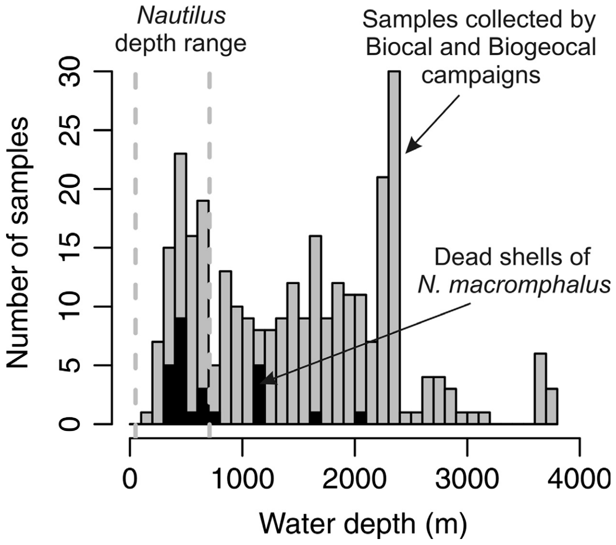

Fig. 5 The bathymetric distribution of dead *N. macromphalus* shells does not follow the overall depth–frequency distribution of *all* grab and dredge collections (i.e. not just collections that contain shells of *N. macromphalus*) sampled during the Biocal and Biogeocal cruises in 1985 and 1987 (grey bars). Individual dead shells of *N. macromphalus* (black bars) were found at water depths largely within the depth range observed for living populations of *N. macromphalus* between 50 and 700 m (grey-dashed vertical lines).

However, the preservation of biostratigraphically condensed ammonites in such settings requires half-lives that significantly exceed the centennial half-lives of Holocene cephalopod shells observed in this study. Early diagenetic precipitation of carbonate cements or lithification of sediment within the shells can be induced by bottom currents and dissolution of unstable carbonate particles (Mullins *et al*., 1980). Such cementation is frequently reported in condensed deposits with hardgrounds (Mutti and Bernoulli, 2003; Preat *et al*., 2011) and with cephalopods (Reolid *et al*., 2010) and can represent a major mechanism that significantly prolongs half-lives. Calcitic foraminifers likely have lower solubility, potentially contributing to their longer half-lives, and thus higher time averaging, relative to aragonitic cephalopods. However, although millennial offsets in the postmortem ages of co-occurring calcitic foraminifers are frequently reported in deep-sea sediments (Broecker *et al*., 1999; Mekik, 2014), the million-year scale half-lives of foraminifers observed here are rather unlikely in the absence of pathways inhibiting disintegration such as burial below the taphonomic active zone followed by exhumation and/or diagenetic stabilisation. Some role of diagenetic cementation in the preservation of extinct foraminifers is implied by coatings rich in coccoliths that completely encase their tests (Fig. 4G) and by moldic preservation of some specimens. Therefore, we suggest that fossil assemblages with chambered cephalopods that lack signs of syndepositional cementation have a very low potential for biostratigraphic condensation.

Nekto-benthic cephalopods have a large potential for significant postmortem transport as shown by accumulations of frequent dead shells of *Nautilus* on the beaches of New Caledonia (Mapes *et al*., 2010a,b; Hembree *et al*., 2014; Seuss *et al*., 2015a,b) and by occurrences that are potentially hundreds of kilometres away from their home range (Reyment, 2008). Even a minor postmortem transport can lead to a significant bathymetric displacement of dead shells in settings with steep topographic gradients. However, the close match between the median depth occurrence of dead *Nautilus* shells at 445 m and the maximum living abundance of *N. macromphalus* between 300 and 400 m (ascending into shallower depths during the night, Ward and Martin, 1980; Roux *et al*., 1991) shows that shells are preserved with excellent bathymetric fidelity relative to their native depth range. *N. macromphalus* inhabits depths between 50 and 700 m; dead shells are rare in samples collected deeper than 800 m. The excellent fidelity in bathymetric maxima thus probably reflects a quick postmortem descent to the seafloor. This is supported by the fact that, out of 26 shells, the body chamber is almost complete in only two specimens and 85–90% complete in six other specimens; most specimens have a highly incomplete or missing body chamber, enhancing waterlogging of the phragmocone. This finding of high bathymetric fidelity is also in accord with modelling and experiments predicting that postmortem water influx can occur at a relatively high rate after mantle detachment (Chamberlain *et al*., 1981; Wani *et al*., 2005) and that a small amount of waterlogging may be needed to counteract the positive buoyancy (Maeda and Seilacher, 1996), particularly at the high hydrostatic pressures at large depths. Negatively buoyant dead shells that sink to depths below their maximum depth limit are probably subject to much higher disintegration rates below the aragonite compensation depth. At such depths, *Nautilus* shells are quickly lost from the basinal seafloor, minimising the mismatch between the bathymetric maxima of living and dead shells.

Conclusions

Dead shells of *Nautilus* generally show very good bathymetric fidelity relative to their living depth range. They exist for only a few hundred years on the seafloor, in contrast to significantly condensed benthic and planktonic calcitic foraminifers. This result is discordant with biostratigraphically condensed fossil cephalopod accumulations observed on pelagic swells in the fossil record. Although *Nautilus* assemblages share some sedimentological and taphonomic similarities with fossil accumulations from sediment-starved pelagic environments, disintegration rates of aragonitic cephalopods in oozes off

New Caledonia are relatively high because, with the exception of goethite-clay coatings, their shells are not significantly strengthened by early-diagenetic seafloor cementation.

Acknowledgements

We thank two reviewers, the associate editor, and Max Coleman for comments, Didier Marchand for introducing us to specimens collected by the Biocal and Biogeocal cruises, Jerome Thomas and Neil Landman for access to specimens deposited at the Université de Bourgogne and the American Museum of Natural History, and Adrián Biroň and Tomáš Mikuš for analytical support. We thank the Slovak Research and Development Agency (0644-10) and the Scientific Slovak Grant Agency (0136-15) for funding, and the 'Centre of Excellence for Integrated Research of Earth's Geosphere' No. ITMS-26220120064, co-financed by ERDF, for support. The AAGL at Northern Arizona University is supported by NSF-EAR-1234413.

References

Allen, A.P., Kosnik, M.A. and Kaufman, D.S., 2013. Characterizing the dynamics of amino acid racemization using time-dependent reaction kinetics: a Bayesian approach to fitting age-calibration models. *Quat. Geochronol.*, **18**, 63–77.

Brayard, A., Bucher, H., Escarguel, G., Fluteau, F., Bourquin, S. and Galfetti, T., 2006. The Early Triassic ammonoid recovery: paleoclimatic significance of diversity gradients. *Palaeogeogr. Palaeoclimatol. Palaeoecol.*, **239**, 374–395.

Broecker, W., Matsumoto, K., Clark, E., Hajdas, I. and Bonani, G., 1999. Radiocarbon age differences between coexisting foraminiferal species. *Paleoceanography*, **14**, 431–436.

Cabioch, G., 2003. Postglacial reef development in the South-West Pacific: case studies from New Caledonia and Vanuatu. *Sed. Geol.*, **159**, 43–59.

Chamberlain, J.A. Jr, Ward, P.D. and Weaver, J.S., 1981. Post-mortem ascent of *Nautilus* shells: implications for cephalopod paleobiogeography. *Paleobiology*, **7**, 494–509.

Chirat, R., 2000. The so-called "cosmopolitan" palaeogeographic distribution of Tertiary Nautilida of the genus *Aturia* Bronn 1838: the result of post-mortem transport by oceanic palaeocurrents. *Palaeogeogr. Palaeoclimatol. Palaeoecol.*, **157**, 59–77.

Coimbra, R. and Olóriz, F., 2012. Contrast comparison of differential diagenetic pathways of Lower Tithonian carbonate materials from the Betic Cordillera (S. Spain): Evidence for physico-chemical paleo-seawater properties. *Palaeogeogr. Palaeoclimatol. Palaeoecol.*, **321–322**, 65–79.

Cotillon, P., Rigolot, P., Coustillas, F., Gaillard, C., Laurin, B., Liu, J.D., Pannetier, W., Pascal, A. and Rio, M., 1989. Pentes et bassins au large de la Nouvelle-Calédonie (Sud-Ouest Pacifique); morphologie, environnements biosédimentaires, sédimentation. *Oceanol. Acta*, **12**, 131–140.

De Forges, B.R., 1990. Les campagnes d'exploration de la faune bathyale dans la zone economique de la Nouvelle-Caledonie. *Resultats des campagnes Musorstom*, **6**, 9–54.

Dera, G., Neige, P., Dommergues, J.-L. and Brayard, A., 2011. Ammonite paleobiogeography during the Pliensbachian-Toarcian crisis (Early Jurassic) reflecting paleoclimate, eustasy, and extinctions. *Global Planet. Change*, **78**, 92–105.

Feely, R.A., Sabine, C.L., Lee, K., Millero, F.J., Lamb, M.F., Greeley, D., Bullister, J.L., Key, R.M., Peng, T.-H., Kozyr, A., Ono, T. and Wong, C.S., 2002. In situ calcium carbonate dissolution in the Pacific Ocean. *Global Biogeochem. Cycles*, **16**, 1144.

Fernández-López, S. and Meléndez, G., 1996. Phylloceratina ammonoids in the Iberian Basin during the Middle Jurassic: a model of biogeographical and taphonomic dispersal related to relative sea-level changes. *Palaeogeogr. Palaeoclimatol. Palaeoecol.*, **120**, 291–302.

Föllmi, K.B., 2016. Sedimentary condensation. *Earth Sci. Rev.*, **152**, 143–180.

Gagan, M.K., Hendy, E.J., Haberle, S.G. and Hantoro, W.S., 2004. Post-glacial evolution of the Indo-Pacific warm pool and El Nino-Southern Oscillation. *Quatern. Int.*, **118**, 127–143.

Hayward, B.W. and Kagawata, S., 2005. Extinct foraminifera figured in Brady's Challenger Report. *J. Micropalaeontol.*, **24**, 171–175.

Hayward, B.W., Kawagata, S., Sabaa, A.T., Grenfell, H.R., Van Kerckhoven, L., Johnson, K. and Thomas, E., 2012. The last global extinction (mid-Pleistocene) of deep-sea benthic foraminifera (Chrysalogoniidae, Ellipsoidinidae, Glandulonodosariidae, Plectofrondiculariidae, Pleurostomellidae, Stilostomellidae), their late Cretaceous-Cenozoic history and taxonomy. *Cushman Found. Foram. Res. Spec. Publ.*, **43**, 1–408.

Hembree, D.I., Mapes, R.H. and Goiran, C., 2014. The impact of high-energy storms on shallow-water *Nautilus* (Cephalopoda) Taphonomy, Lifou (Loyalty islands). *Palaios*, **29**, 348–362.

Henderson, R.A. and McNamara, K.J., 1985. Taphonomy and ichnology of cephalopod shells in a Maastrichtian chalk from Western Australia. *Lethaia*, **18**, 305–322.

Kaufman, D.S. and Manley, W.F., 1998. A new procedure for determining DL amino acid ratios in fossils using reverse phase liquid chromatography. *Quatern. Sci. Rev.*, **17**, 987–1000.

Kennett, J. and Srinivasan, M.S., 1983. *Neogene Planktonic Foraminifera – A Phylogenetic Atlas*. Hutchinson Ross, Stroudsburg, Pennsylvania.

Kidwell, S.M., Best, M.M.R. and Kaufmann, D.S., 2005. Taphonomic trade-offs in tropical marine death assemblages: differential time averaging, shell loss, and probable bias in siliciclastic vs. carbonate facies. *Geology*, **33**, 729–732.

Kosnik, M.A. and Kaufman, D.S., 2008. Identifying outliers and assessing the accuracy of amino acid racemization measurements for geochronology: II. Data screening. *Quat. Geochronol.*, **3**, 328–341.

Landman, N.H., Mapes, R.H., Cochran, J.K., Lignier, V., Hembree, D.I., Goiran, C., Folcher, E. and Brunet, P., 2014. An unusual occurrence of *Nautilus macromphalus* in a Cenote in the Loyalty Islands (New Caledonia). *PLoS ONE*, **9**, e113372.

Maeda, H., 1991. Sheltered preservation: a peculiar mode of ammonite occurrence in the Cretaceous Yezo Group, Hokkaido, north Japan. *Lethaia*, **24**, 69–82.

Maeda, H. and Seilacher, A., 1996. Ammonoid taphonomy. In: *Ammonoid Paleobiology* (N. Landman, N. Landman, R.A. Davis, eds), pp. 543–578. Plenum Press, New York.

Mapes, R.H., Landman, N.H., Cochran, K., Goiran, C., De Forges, B.R. and Renfro, A., 2010a. Early taphonomy and significance of naturally submerged *Nautilus* shells from the New Caledonia region. *Palaios*, **25**, 597–610.

Mapes, R.H., Hembree, D.I., Rasor, B.A., Stigall, A., Goirand, C. and De Forges, B.R., 2010b. Modern *Nautilus* (Cephalopoda) taphonomy in a subtidal to backshore environment, Lifou (Loyalty Islands). *Palaios*, **25**, 656–670.

Martin-Algarra, A. and Sanchez-Navas, A., 1995. Phosphate stromatolites from condensed cephalopod limestones, Upper Jurassic, Southern Spain. *Sedimentology*, **42**, 893–919.

Martire, L., 1996. Stratigraphy, facies and synsedimentary tectonics in the Jurassic Rosso Ammonitico Veronese

(Altopiano di Asiago, NE Italy). *Facies*, **35**, 209–236.

Mekik, F., 2014. Radiocarbon dating of planktonic foraminifer shells: a cautionary tale. *Paleoceanography*, **29**, 13–29.

Mullins, H.T., Neumann, A.C., Wilber, R.J. and Boardman, M.R., 1980. Nodular carbonate sediment on Bahamian slopes: possible precursors to nodular limestones. *J. Sediment. Petrol.*, **50**, 117–131.

Mutti, M. and Bernoulli, D., 2003. Early marine lithification and hardground development on a Miocene ramp (Maiella, Italy): key surfaces to track changes in trophic resources in montropical carbonate settings. *J. Sediment. Res.*, **73**, 296–308.

Olszewski, T.D. and Kaufman, D.S., 2015. Tracing burial history and sediment recycling in a shallow estuarine setting (Copano Bay, Texas) using postmortem ages of the bivalve *Mulinia lateralis*. *Palaios*, **30**, 224–237.

Pavia, G., Defaveri, A., Maerten, L., Pavia, M. and Zunino, M., 2013. Ammonite taphonomy and stratigraphy of the Bajocian at Maizet, south of Caen (Calvados, NW France). *C.R. Palevol*, **12**, 137–148.

Powell, E.N., Brett, C.E., Parsons-Hubbard, K.M., Callender, W.R., Staff, G.M., Walker, S.E., Raymond, A. and Ashton-Alcox, K.A., 2011. The relationship of bionts and taphonomic processes in molluscan taphofacies formation on the continental shelf and slope: Eight-year trends: Gulf of Mexico and Bahamas. *Facies*, **57**, 15–37.

Preat, A., Mamet, B., Di Stefano, P., Martire, L. and Kolo, K., 2011. Microbially-induced Fe and Mn oxides in condensed pelagic sediments (Middle-Upper Jurassic, Western Sicily). *Sed. Geol.*, **237**, 179–188.

Reolid, M., Nieto, L.M. and Rey, J., 2010. Taphonomy of cephalopod assemblages from Middle Jurassic hardgrounds of pelagic swells (South-Iberian Palaeomargin, Western Tethys). *Palaeogeogr. Palaeoclimatol. Palaeoecol.*, **292**, 257–271.

Reyment, R.A., 2008. A review of the post-mortem dispersal of cephalopod shells. *Palaeontol. Electron.*, **11**, 13.

Roux, M., Bouchet, P., Bourseau, J.-P., Gaillard, C., Grandperrin, R., Guille, A., Laurin, B., Monniot, C., De Forges, B.R., Rio, M., Segonzac, M., Vacelet, J. and Zibrowius, H., 1991. L'environnement bathyal au large de la Nouvelle-Calédonie: résultats préliminaires de la campagne CALSUB et conséquences paléoécologiques. *Bull. Soc. Géol. Fr.*, **162**, 675–685.

Santantonio, M. and Carminati, E., 2011. Jurassic rifting evolution of the Apennines and Southern Alps (Italy): parallels and differences. *Geol. Soc. Am. Bull.*, **123**, 468–484.

Sessa, J.A., Larina, E., Knoll, K., Garb, M., Cochran, J.K., Huber, B.T., MacLeod, K.G. and Landman, N.H., 2015. Ammonite habitat revealed via isotopic composition and comparisons with co-occurring benthic and planktonic organisms. *Proc. Natl Acad. Sci.*, **112**, 15562–15567.

Seuss, B., Hembree, D.I., Wisshak, M., Mapes, R.H. and Landman, N.H., 2015a. Taphonomy of deep-marine versus backshore collected *Nautilus macromphalus* conchs (New Caledonia). *Palaios*, **30**, 503–513.

Seuss, B., Wisshak, M., Mapes, R.H. and Landman, N.H., 2015b. Syn-vivo bioerosion of *Nautilus* by endo-and epilithic foraminiferans (New Caledonia and Vanuatu). *PLoS ONE*, **10**, e0125558.

Stuiver, M. and Reimer, P.J., 1993. Extended 14C data base and revised CALIB 3.0 C age calibration program. *Radiocarbon*, **35**, 215–230.

Terry, R.C. and Novak, M., 2015. Where does the time go?: mixing and the depth-dependent distribution of fossil ages. *Geology*, **43**, 487–490.

Thompson, P.R., Bé, A.W.H., Duplessy, J.-C. and Shackleton, N.J., 1979. Disappearance of pink-pigmented *Globigerinoides ruber* at 120,000 yr BP in the Indian and Pacific oceans. *Nature*, **280**, 554–558.

Tomašových, A., Kidwell, S.M., Foygel Barber, R. and Kaufman, D.S., 2014. Long-term accumulation of carbonate shells reflects a 100-fold drop in loss rate. *Geology*, **42**, 819–822.

Tomašových, A., Kidwell, S.M. and Foygel Barber, R., 2016. Inferring skeletal production from time-averaged assemblages: skeletal loss pulls the timing of production pulses towards the modern period. *Paleobiology*, **42**, 54–76. dx.doi.org/10.1017/pab.2015.30.

Wani, R., Kase, T., Shigeta, Y. and De Ocamp, R., 2005. New look at ammonoid taphonomy, based on field experiments with modern chambered *Nautilus. Geology*, **33**, 849–852.

Ward, P.D. and Martin, A.W., 1980. Depth distribution of *Nautilus pompilius* in Fiji and *Nautilus macromphalus* in New Caledonia. *Veliger*, **22**, 259–264.

Wendt, J. and Aigner, T., 1985. Facies patterns and depositional environments of Palaeozoic cephalopod limestones. *Sed. Geol.*, **44**, 263–300.

Received 30 October 2015; revised version accepted 15 April 2016

Supporting Information

Additional Supporting Information may be found in the online version of this article:

Data S1. Methods – age calibration.

Data S2. Differences between the prismatic and nacreous layer.

Data S3. Shell preservation

Data S4. Last appearances of foraminifers.

Figure S1. Location of stations where dead shells of *Nautilus macromphalus* were collected for this study.

Figure S2. Data screening. (A) L-serine concentrations ([L-Ser]) relative to glutamic acid concentrations ([D+L Glu]) against aspartic acid (Asp) D/L. (B) Concentrations of Asp relative to Glu. (C) Asp D/L relative to Glu D/L, showing that Asp is more racemised in the prismatic layer.

Figure S3. Top row: Relation between postmortem age (determined by 14C and 210Pb) and D/L values of two amino acids for the prismatic and nacreous layers, best-fit by TDK1 and CPK0 models, respectively, representing the best fits on the basis of BIC, and assuming log-normal and gamma distributions for the residuals.

Figure S4. Top row: Box-and-whisker plots showing the concentrations and relative abundances of eight amino acids in the prismatic and nacreous layers.

Figure S5. Cross-section photomicrographs of the external prismatic and the middle nacreous layer showing a higher degree of microbioerosion in the external prismatic layer (upper part) than in the thicker nacreous layer.

Figure S6. Incomplete relicts are significantly older than specimens with complete phragmocones.

Table S1. Geographic coordinates and water depths of 26 specimens of *Nautilus macromphalus*, with information on the presence of extinct foraminifers (with times of their last appearance).

Table S2. Radiocarbon (and ^{210}Pb for the specimen 55924) ages used to calibrate the rate of amino acid racemisation. Specimen ages refer to 2014 when amino acid composition was completed.

Table S3. Calibration statistics for the rate of amino acid racemisation (AAR) based on paired AAR and radiometric analyses of *Nautilus macromphalus* and two models of uncertainty.

Table S4. Postmortem ages used in the construction of age–frequency distribution (relative to time since collection of shells on the sea-floor) with the corresponding D/L values for the external spherulitic-prismatic layer and the middle nacreous layer.

Table S5. Parameters of three models (one-phase exponential, Weibull, and two-phase exponential model) fitted to two age–frequency distributions, with AIC and BIC values.

Table S6. Foraminifers found in ooze sediments within whorls of 14 shells.

Table S7. Concentrations of amino acids in the prismatic and nacreous layers.